Supplement Information of "Onset of the Quantum Hall Effect at 5 mT in Double-Layer Graphene"

Alexander S. Mayorov[1,b)], Ping Wang[1,b)], Xiaokai Yue[2,b)], Biao Wu[1], Jianhong He[3], Di Zhang[1], Fuzhuo Lian[1], Siqi Jiang[1], Jiabei Huang[1], Zihao Wang[4], Qian Guo[5,6], Kenji Watanabe[7], Takashi Taniguchi[8], Renjun Du[1], Rui Wang[1], Jie Gao[2,3],Baigeng Wang[1,10,11,a)], Lei Wang[1,9,10,11,a)], Kostya S. Novoselov[4,a)], and Geliang Yu[1,9,10,11,a)]

[1]National Laboratory of Solid State Microstructures, School of Physics, Nanjing University, Nanjing 210093, China
[2]Department of Physics, Sichuan Normal University, Chengdu, Sichuan 610066, China
[3]College of Physics, Sichuan University, Chengdu, Sichuan 610064, China
[4]Institute for Functional Intelligent Materials, National University of Singapore, Singapore
[5]Department of Physics and Astronomy, University of Manchester, Manchester, UK
[6]National Graphene Institute, University of Manchester, Manchester, UK
[7]Research Center for Functional Materials, National Institute for Material Science, 1-1 Namiki, Tsukuba 305-0044, Japan
[8]International Center for Materials Nanoarchitectonics, National Institute for Material Science, 1-1 Namiki, Tsukuba 305-0044, Japan
[9]International Joint Laboratory on Two Dimensional Materials, Nanjing University, Nanjing,China
[10]Collaborative Innovation Center of Advanced Microstructures, Nanjing University, Nanjing,China
[11]Jiangsu Physical Science Research Center, Nanjing, China.
[a)]Authors to whom any correspondence should be addressed:bgwang@nju.edu.cn, leiwang@nju.edu.cn, kostya@nus.edu.sg and yugeliang@nju.edu.cn
[b)]These authors contributed equally to this work.

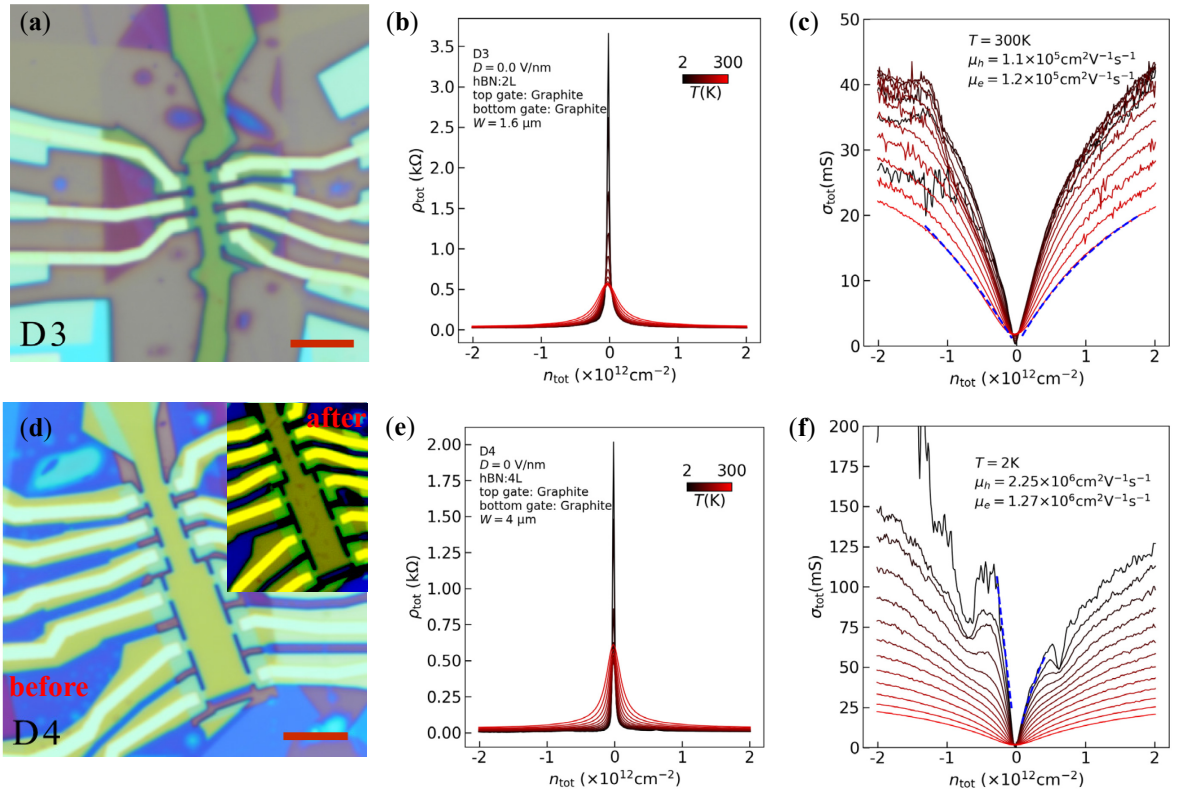

FIG S1. (**a**) The optical image of device D3. (**b**) The resistivity of D3 as a function of n_{tot} and T. (**c**) The total conductivity as a function of n_{tot} and T, the field effect mobility of holes and electrons at $T = 300\mathrm{K}$ are extracted by fitting as the dashed lines via $\sigma_{\mathrm{tot}}^{-1} = (n_{\mathrm{tot}} e\mu_{EF} + \sigma_{\mathrm{min}})^{-1} + \rho_s$, σ_{min} is the smallest conductivity at the CNP, ρ_s is resistivity led by the short-range scattering.[1,2] (**d**) The optical image of device D4. While attempting to observe quantum effects at room temperature, a rapid cooling down and warming up resulted in some dirty bubbles on the surface as shown in the upper right inset. (**e-f**) After the surface of D4 became dirty, the maximum resistivity was found to be only 2 kΩ, which is significantly smaller than that of the other devices without surface contamination. However, the resistance peaks remain steep, and the mobility at 2 K also reaches 10^6 $\mathrm{cm^2V^{-1}s^{-1}}$. The surface contamination only affects the doping of the upper layer graphene, resulting in a reduced maximum resistivity, while leaving the lower graphene unaffected, thus ensuring high mobility. The scale bars are 5 μm.

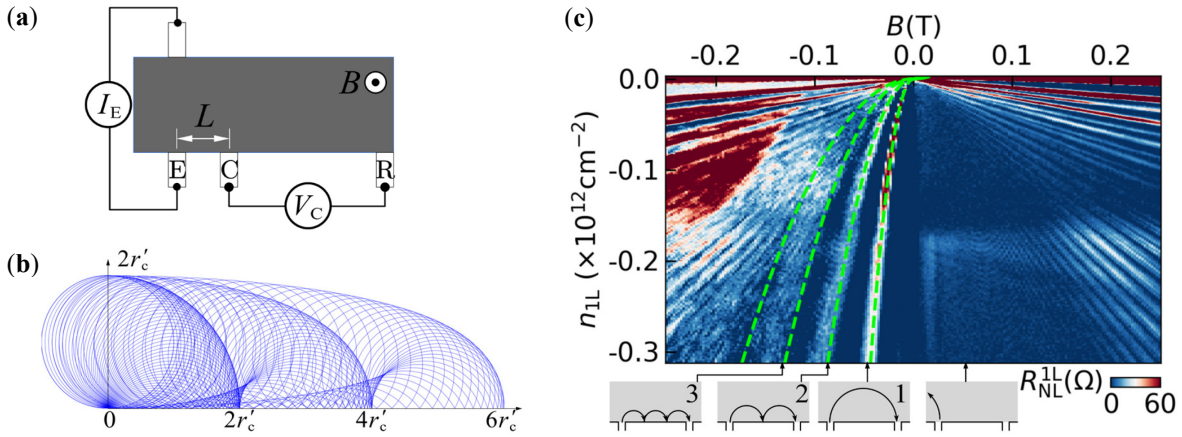

FIG S2. (**a**) Nonlocal connection for transverse magnetic focusing effect measurement.[3,4] Contact E injects current I_E into DLG, and the voltage V_C is measured at the collector (contact C) relative to contact R. The distance between the centers of contacts E and C is L. (**b**) Classical trajectories of electrons injected isotropically from the origin at $B' = 3B_f$. Electrons are focused at an integer multiple of $2r_c'$ along Ldirection. (**c**) TMF spectrum in D2 at $D = 0$ V/nm and $T = 15$ mK, where $R_{NL}^{1L} = 2R_{NL}^{tot}$ and $n_{1L} = n_{tot}/2$ as decoupled parallel two layers. TMF oscillations at the hole side B_1, B_2, B_3 (as shown by lime green dashed lines) were observed clearly for $|B| < 0.2$ T. The dashed lines are calculated using $B_j = (2j\hbar/\pm eL)\sqrt{\pi|n_{1L}|}$, $j = 1,2,\cdots$. The bottom insets show representative trajectories for each corresponding mode.

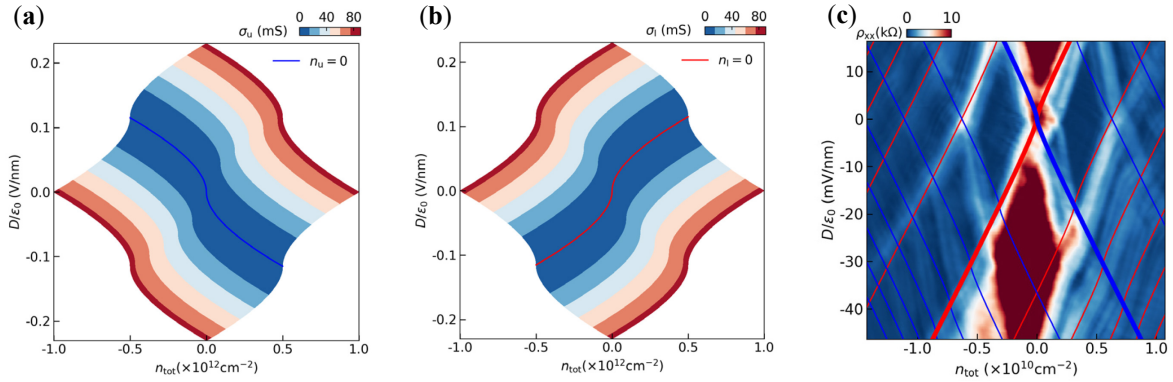

FIG S3. (**a-b**) Computed conductivity of the upper (a) and lower (b) graphene layer in the (n_{tot}, D) space, respectively. (**c**) Identify the corresponding filling factors from the experimental result.

Dual-gated DLG allows obtaining the individual carrier density in each layer n_{u} and n_{l} at arbitrary values of the applied gate voltage V_{tg} and V_{bg}. To extract the filling factor from Fig 3(a), we employ the following procedure:

1. Take a dense sequence of equally spaced values of n_{upper} and n_{lower} over our experimentally relevant range, e.g. $n_{\mathrm{u}} = n_{\mathrm{l}} = [-0.5, 0.5] \times 10^{12}\mathrm{cm}^{-2}$, and transform n_{u} and n_{l} into a two-dimensional data grid $(n_{\mathrm{u}}, n_{\mathrm{l}})$.
2. In the $(n_{\mathrm{u}}, n_{\mathrm{l}})$ space, via the equation $D = C_{\mathrm{m}}(\Delta\mu/e) + e\Delta n/2$, to calculate D, and $n_{\mathrm{tot}} = n_{\mathrm{u}} + n_{\mathrm{l}}$, now we have got the $n_{\mathrm{tot}} - D$ space.
3. In the $n_{\mathrm{u}} - n_{\mathrm{l}}$ space, calculate the σ_{u} and σ_{l} via the equations $\sigma_{\mathrm{u}} = (n_{\mathrm{u}}, 0)e\mu_{FE}$ and $\sigma_{\mathrm{l}} = (0, n_{\mathrm{l}})e\mu_{FE}$, respectively, here we set the mobility as $\mu_{FE} = 1 \times 10^{6}\ \mathrm{cm}^2\mathrm{V}^{-1}\mathrm{s}^{-1}$. Plot σ_{u} in the $n_{\mathrm{tot}} - D$ space as shown in Fig S3(a). The same for the lower layer as shown in Fig S3(b).

When a magnetic field is present, all the states are organized into Landau levels (LLs), and the energy level spacing is given by $E_N = \pm v_F\sqrt{2\hbar eBN}, N \in \mathbb{Z}$. For monolayer graphene, the corresponding filling sequence is $\nu = \pm 4(N + 1/2)$ with spin and valley degeneracy. In Fig S3(a), the same color indicates that within this $\sigma_{\mathrm{u}}(n_{\mathrm{u}})$ range has the same $|\nu_{\mathrm{u}}|$. Noting that electrons exhibit positive filling factors while holes exhibit negative filling factors, one must also consider the signs of the filling factors on both sides of the CNP. By comparing with experimental results, we can figure out the LLs intersecting shown in Fig S3(c).

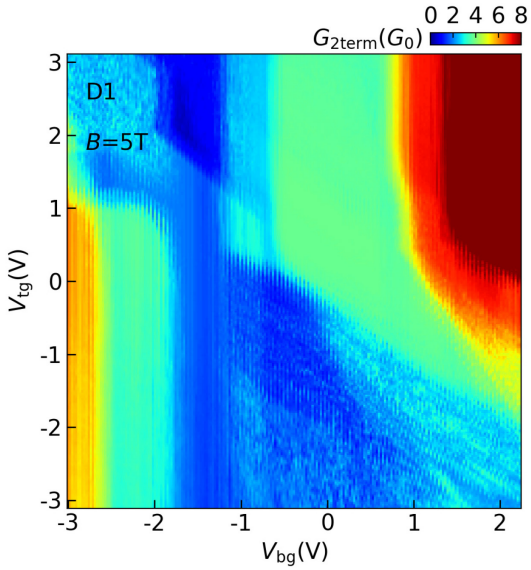

FIG S4. The two-terminal conductance of device D1 with Type I ohmic contacts was measured at $B = 5$T. The top gate and the channel are not aligned, resulting in a significant p-n junction effect[5] at a magnetic field of 5 T.

Mobility

From the Feynman diagram in Fig.2c, the renormalized interactions are calculated via the following Dyson equation[6]

$$\begin{pmatrix} W_{11} & W_{12} \\ W_{21} & W_{22} \end{pmatrix} = \begin{pmatrix} V_{11} & V_{12} \\ V_{21} & V_{22} \end{pmatrix} + \begin{pmatrix} V_{11} & V_{12} \\ V_{21} & V_{22} \end{pmatrix} \begin{pmatrix} \Pi_1 & 0 \\ 0 & \Pi_2 \end{pmatrix} \begin{pmatrix} W_{11} & W_{12} \\ W_{21} & W_{22} \end{pmatrix},$$

where W is the screened Columb interaction and Π_1, Π_2 are the polarization functions given by the fermion bubble diagram. By solving the matrix equation, $\widehat{W} = \left(1 - \hat{V}\hat{\Pi}\right)^{-1}\hat{V}$, we can obtain the screened intralayer Columb interaction (taking layer 1 as an example), $W_{11} = V_{11}/\varepsilon$, where the effective dielectric function is found as[6]

$$\varepsilon^{-1} = \frac{1-\Pi_2(V_{22}-V_{12}V_{21}/V_{11})}{(1-V_{11}\Pi_1)(1-V_{22}\Pi_2)-V_{12}V_{21}\Pi_1\Pi_2}.$$

It is noted that for $d \to \infty$, the effective dielectric function becomes $\varepsilon^{-1} = 1 - V_{11}\Pi_1$, which is reduced to that of the single-layer graphene.

In our calculation, the static polarizability is obtained at zero temperature[7,8], i.e.,

$$\Pi_i = -\frac{2k_{Fi}}{\pi\hbar v_F}\left[\Theta(2k_{Fi}-q) + \left(1 + \frac{\pi q}{8k_{Fi}} - \frac{1}{2}\sqrt{1-\frac{4k_{Fi}^2}{q^2}} - \frac{q}{4k_{Fi}}sin^{-1}\frac{2k_{Fi}}{q}\right)\Theta(q-2k_{Fi})\right]$$

where $k_{Fi} = \sqrt{\pi n_i}$ is the Fermi wave vector of the ith layer graphene, and n_i stands for its carrier density. In the case where the Columb scattering, the scattering time dominates the transport properties of graphene τ (of layer 1) at $T = 0$ that determines the conductivity satisfies[6]

$$\frac{\hbar}{\tau} = \frac{n_{imp}}{4\pi} \int d\boldsymbol{k}' \left[\frac{V_{11}(|\boldsymbol{k}-\boldsymbol{k}'|)}{\varepsilon(|\boldsymbol{k}-\boldsymbol{k}'|)}\right]^2 [1-\cos^2(\theta)]\delta(E_{k'} - E_k),$$

where $q = |\boldsymbol{k} - \boldsymbol{k}'| = 2k_F \sin(\theta/2)$ is the transfer momentum and n_{imp} is the charge impurity density. Finally, the mobility can be obtained from $\mu = \sigma/ne = 2ev_F k_F \tau/\hbar n$. Due to the enhanced screening, the scattering time τ is enlarged, which significantly enhances the mobility of the sample. Compared to the single-layer case, we find that μ. The double-layer structure is generally enhanced by 2 or 3 times compared to the single-layer case. Fig S5 shows more detailed data for different impurity densities and layer separations.

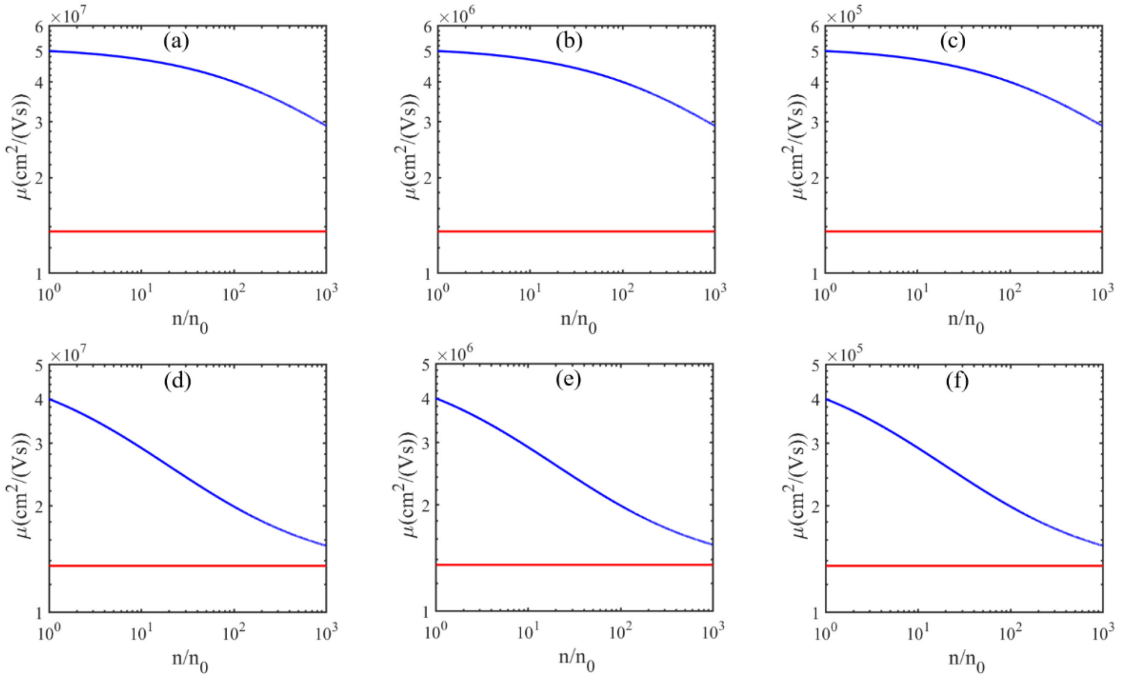

FIGS.S5 The mobility per layer as a function of the carrier density $n_1 = n_2 = n$ ($n_0 = 10^7\ cm^{-2}$) for different layer separations and impurity densities. The red line and blue curves represent the single-layer and double-layer graphene cases, respectively. $d = 1\ nm$ in (**a-c**), and $d = 10\ nm$ in (**e-f**). The charge impurity density $n_{imp} = 2 \times 10^8\ cm^{-2}$ in (**a**) (**d**), $n_{imp} = 2 \times 10^9\ cm^{-2}$ in (**b**) (**e**) and $n_{imp} = 2 \times 10^{10}\ cm^{-2}$ in (**c**) (**f**). It is clearly shown that the mobility enhancement would be more significant for lower carrier densities and smaller layer separations.

REFERENCES

1. Das Sarma, S., Adam, S., Hwang, E. H. & Rossi, E. Electronic transport in two-dimensional graphene. *Rev. Mod. Phys.* **83**, 407–470 (2011).
2. Mayorov, A. S. *et al.* How Close Can One Approach the Dirac Point in Graphene Experimentally? *Nano Lett.* **12**, 4629–4634 (2012).
3. Berdyugin, A. I. *et al.* Minibands in twisted bilayer graphene probed by magnetic focusing. *Sci. Adv.* **6**, 7838 (2020).
4. Taychatanapat, T., Watanabe, K., Taniguchi, T. & Jarillo-Herrero, P. Electrically tunable transverse magnetic focusing in graphene. *Nature Phys* **9**, 225–229 (2013).
5. Amet, F., Williams, J. R., Watanabe, K., Taniguchi, T. & Goldhaber-Gordon, D. Selective Equilibration of Spin-Polarized Quantum Hall Edge States in Graphene. *Phys. Rev. Lett.* **112**, 196601 (2014).
6. Kechedzhi, K., Hwang, E. H. & Sarma, S. D. Gate-tunable quantum transport in double-layer graphene. *Phys. Rev. B* **86**, 165442 (2012).
7. Hwang, E. H. & Das Sarma, S. Dielectric function, screening, and plasmons in two-dimensional graphene. *Phys. Rev. B* **75**, 205418 (2007).
8. Adam, S., Hwang, E. H., Galitski, V. M. & Sarma, S. D. A self-consistent theory for graphene transport. *PANS* **104**, 18392–18397 (2007).